Journal of Inflammation Research

Dovepress
Taylor & Francis Group

Open Access Full Text Article

ORIGINAL RESEARCH

Exploring Immunological Determinants and Constructing a Predictive Model for Diagnosis of Gout: Insights Into Immune Biomarkers

Huanhuan Zeng*, Liqiang Zheng*, Dan Wu, Xiang Yu, Guangjiang Zhang, Jinwan Du

Department of Rheumatology and Immunology, People's Hospital of Chongqing Liangjiang New Area, Chongqing, 401121, People's Republic of China

*These authors contributed equally to this work

Correspondence: Jinwan Du, Department of Rheumatology and Immunology, People's Hospital of Chongqing Liangjiang New Area, No. 2, Jinkai Avenue, Yubei District, Chongqing, 401121, People's Republic of China, Email qq88552071@163.com

Introduction: Immune-inflammatory mechanisms play a pivotal role in gout pathogenesis, yet the specific immunological signatures and their predictive utility remain underexplored.

Methods: This cross-sectional study enrolled 130 participants (65 gout patients, 65 controls) to compare clinical characteristics, inflammatory markers, and immune profiles. Key variables were selected via least absolute shrinkage and selection operator (LASSO) regression, and an extreme gradient boosting (XGBoost) prediction model was constructed. Model interpretability and robustness were assessed using SHapley Additive exPlanations (SHAP), principal component analysis (PCA), and external validation.

Results: Baseline characteristics showed no significant intergroup differences, ensuring cohort comparability. Gout patients exhibited elevated levels of inflammatory mediators, including C-reactive protein (CRP), high-sensitivity CRP (hs-CRP), interleukin-1β (IL-1β), interleukin-6 (IL-6), and NLR family pyrin domain-containing 3 (NLRP3), alongside immune dysregulation marked by increased $CD4^+$/$CD8^+$ and Th17/regulatory T-cell (Treg) ratios and $CD14^+$/$CD16^+$ monocyte expansion, indicating systemic inflammatory activation and immune imbalance. Cluster analysis identified two immunological subtypes. The XGBoost model, incorporating seven LASSO-selected biomarkers, achieved perfect discrimination in internal validation (AUC = 1.0, accuracy = 100%) and high performance in an external cohort (AUC = 0.977, accuracy = 93.75%). PCA and random forest analyses confirmed hs-CRP and IL-1β as core predictors.

Conclusion: Gout is characterized by distinct immune-inflammatory signatures. The machine learning model leveraging immunological biomarkers demonstrates exceptional classification accuracy and generalizability, offering potential for early screening and immunological subtyping in clinical practice, may support earlier diagnosis in patients with atypical or silent gout manifestations.

Keywords: gout, immune biomarkers, inflammation, LASSO regression, XGBoost model, immunological subtyping, predictive model, principal component analysis, random forest

Introduction

Gout is a metabolic disorder characterized by the deposition of monosodium urate crystals, primarily manifesting as recurrent acute arthritis. In severe cases, complications such as tophi formation, chronic joint deformities, and renal impairment may occur.[1,2] Driven by lifestyle modifications and the widespread consumption of high-purine diets, the global incidence of gout has risen persistently, emerging as a critical public health concern affecting middle-aged and elderly populations.[3] Although hyperuricemia is strongly associated with gout pathogenesis, accumulating evidence indicates that only a subset of individuals with hyperuricemia progress to clinical gout, suggesting a pivotal role for immune-inflammatory mechanisms alongside metabolic dysregulation in disease progression.[4] Globally, the prevalence of gout has risen steadily, with an estimated 652 per 100,000 individuals affected in 2019, and projections suggesting nearly 100 million patients by 2050.[5,6] Prevalence varies considerably by region, ranging from over 1400 per 100,000 in high-income regions such as North America and Oceania to below 250 per 100,000 in Central America and the Caribbean.[7]

Received: 24 June 2025
Accepted: 6 October 2025
Published: 23 October 2025

Recent advances have elucidated the involvement of immune components, including inflammasomes, inflammatory cytokines, and T-cell subsets, in gout pathogenesis.[8] Notably, activation of the NLR family pyrin domain-containing 3 (NLRP3) inflammasome drives interleukin-1β (IL-1β) release, triggering hallmark acute inflammatory responses.[9–11] Elevated expression of cytokines such as interleukin-6 (IL-6) and tumor necrosis factor-α (TNF-α) further underscores their contributory roles.[12,13] Additionally, immune dysregulation, marked by Th17/regulatory T-cell (Treg) imbalance, abnormal $CD4^+/CD8^+$ ratios, and proinflammatory monocyte phenotypes, is frequently observed in gout patients.[14,15] These findings provide novel insights into the immunological underpinnings of gout. However, current research predominantly focuses on isolated immune markers, failing to systematically integrate multifactorial immune signatures or establish comprehensive models for quantifying and predicting gout risk.

Current clinical practice lacks individualized risk prediction tools based on immune profiles for gout, relying instead on serum uric acid levels and symptomatic evaluation, an approach limited by diagnostic delays and challenges in identifying subtype-specific populations.[16] Although serum uric acid is widely used in clinical practice, it is not a reliable diagnostic marker. Many patients experience normal uric acid levels during acute flares, and nearly half of patients with asymptomatic hyperuricemia never progress to gout.[17] These limitations highlight the need for more sensitive and specific immunological biomarkers.[1] Furthermore, the heterogeneous immunophenotypes of gout, ranging from acute episodic to chronic progressive forms, remain inadequately classified using conventional methods. There is thus an urgent need to develop integrative predictive models that reflect inflammatory status, immune dysregulation, and disease trajectories to enable early identification and personalized intervention.

However, the primary concern for patients with gout lies in its often silent yet progressive course toward tophaceous gout and related complications, including joint deformity, chronic pain, and disability. Despite its clinical burden, many patients remain underdiagnosed or misdiagnosed.[18] This is partly due to challenges in recognizing gout in its early or atypical stages. Elderly patients may fail to recall or report transient flares, leading to missed clinical cues. Radiological findings are frequently nonspecific or misinterpreted, while dual-energy computed tomography (DECT),[19,20] though valuable, has limitations in detecting small urate deposits owing to imaging artifacts and remains inaccessible in many clinical settings.[21,22] Similarly, the gold standard of urate crystal identification via joint aspiration is invasive, technically demanding, and not always feasible in routine practice. These diagnostic gaps contribute to delayed treatment initiation, increased risk of tophi formation, and higher incidence of comorbidities such as cardiovascular disease and chronic kidney disease. Therefore, there is an urgent need to establish practical, cost-effective, and widely applicable diagnostic strategies with both high sensitivity and specificity. Such approaches would not only improve early disease recognition but also facilitate timely intervention, reduce long-term complications, and ultimately enhance patient outcomes.

Despite serum uric acid being the clinical cornerstone, only a fraction of hyperuricemic patients develop gout, highlighting marked disease heterogeneity. Both innate immunity (eg, NLRP3 inflammasome activation, IL-1β release) and adaptive immunity (eg, Th17/Treg imbalance) contribute to pathogenesis. Conventional statistical approaches fail to integrate such multifactorial signatures, whereas machine learning can capture nonlinear interactions and stratify patients into immunological subtypes. This precision approach may ultimately support individualized interventions, such as guiding IL-1β versus IL-6 targeted therapy. To address these gaps, this study systematically analyzes immune signatures in gout patients to identify key biomarkers. A risk prediction model will be constructed using the least absolute shrinkage and selection operator (LASSO) and extreme gradient boosting (XGBoost) algorithms, with further optimization via principal component analysis (PCA) and random forest (RF) algorithm. Concurrently, cluster analysis will delineate immune subtypes of gout to inform precision management strategies. This work aims to provide novel frameworks for early screening, immune risk stratification, and tailored clinical interventions, advancing both research and practical applications in gout management. To our knowledge, this study is among the first to integrate immune biomarkers with machine learning to construct a predictive model for gout. This approach not only provides methodological novelty but also offers a potential framework for stratified diagnosis and individualized treatment.

Materials and Methods

Sample Collection and Processing

This cross-sectional study was conducted in accordance with the ethical principles of the Declaration of Helsinki and approved by the Ethics Committee of the People's Hospital of Chongqing Liang Jiang New Area (Approval No.: 2025–066). Participants included 65 hospitalized gout patients (experimental group, patients were hospitalized mainly due to acute flares or gout-related complications) and 65 age- and sex-matched controls (control group, control participants were defined as individuals free of rheumatic and metabolic diseases, with common chronic conditions excluded) underwent physical examination in the People's Hospital of Chongqing Liang Jiang New Area between January 2023 and December 2024. Participant privacy and personal data were rigorously protected, with all information exclusively used for research purposes. An external validation cohort consisting of 48 patients was recruited between 2023 and 2024, using the same inclusion and exclusion criteria as the discovery cohort.

Gout diagnosis adhered to the guidelines for gout diagnosis and management by the Chinese Society of Rheumatology, Chinese Medical Association.[23,24] Diagnosis required fulfillment of at least two of the following criteria: (1) recurrent acute monoarthritis with erythema, swelling, heat, and pain, typically involving the first metatarsophalangeal joint; (2) hyperuricemia (serum uric acid > 420 μmol/L in males or > 360 μmol/L in females); (3) clinically or radiologically detectable tophi; (4) monosodium urate crystals identified in synovial fluid via polarized light microscopy; or (5) urate crystal deposition in joints and surrounding tissues confirmed by imaging modalities such as ultrasound or dual-energy computed tomography (DECT). All diagnoses were independently validated by two senior rheumatologists.

Sample size estimation was performed using a two-independent-sample mean comparison method. Based on preliminary experiments identifying IL-1β as a critical inflammatory marker, a standardized effect size of 0.7 between groups was assumed. With two-tailed $\alpha = 0.05$, $\beta = 0.10$ (90% power), and PASS software analysis, the minimum required sample size per group was 58. Accounting for a 10% attrition rate, 65 participants per group were enrolled to ensure statistical robustness.

Inclusion criteria were as follows: (1) age ≥ 18 years; (2) for the gout group: fulfillment of ≥ 2 diagnostic criteria outlined in the latest guidelines for gout diagnosis and management by the Chinese Society of Rheumatology, Chinese Medical Association (typical clinical manifestations, hyperuricemia, tophi, urate crystals, or imaging evidence); (3) for controls: physical examination participants or volunteers who had no gout or rheumatic diseases with normal serum uric acid levels; (4) voluntary participation with informed consent.

Exclusion criteria included: (1) comorbid rheumatic disorders (eg, rheumatoid arthritis, systemic lupus erythematosus, psoriatic arthritis); (2) severe hepatic/renal insufficiency, malignancies, or hematologic diseases; (3) acute infections, major trauma, or postoperative recovery phases potentially affecting inflammatory markers; (4) cognitive impairment, psychiatric disorders, or inability to complete study procedures; (5) pregnancy or lactation.

This non-interventional observational study investigated immune factors in gout and developed an early prediction model. Participants comprised gout patients and controls, with all samples and data sourced from existing clinical databases and biorepositories at our hospital. No additional clinical interventions, pharmacological treatments, or follow-up procedures were implemented, ensuring no incremental risk to subjects. Baseline comorbidity data, including hypertension, diabetes mellitus, and hyperlipidemia, were collected from medical records. Medication history was also reviewed, with particular attention to the use of diuretics, nonsteroidal anti-inflammatory drugs (NSAIDs), and antihypertensive agents.

The samples of the control group consisted of de-identified remnant blood specimens from routine health examinations conducted by our Medical Examination Center and Clinical Laboratory, supplemented by anonymized historical data from health databases. No additional sample collection or interventions were performed for this study. Prior to analysis, all datasets underwent rigorous de-identification, with personally identifiable information, including names, national ID numbers, contact details, and accession numbers, permanently removed. Processed samples and data were exclusively utilized for immune factor quantification and statistical modeling without individual traceability. Participants underwent no additional phlebotomy, diagnostic procedures, or follow-up, with no impact on their diagnosis and treatment behaviors or daily activities. Given the anonymous nature of pre-existing samples and the operational impracticability of retrospective consent acquisition, coupled with the minimal-risk status of this study, the Ethics Committee granted a waiver of informed consent for the controls.

The data of the gout group were derived from electronic medical records of outpatient and inpatient services in the Department of Rheumatology and Immunology and the Department of Endocrinology of our hospital. Serum samples represented clinical remnants from prior diagnostic testing. No supplemental sampling, investigations, or therapeutic modifications were introduced. Extracted clinical data maintained strict anonymization, retaining only research-relevant variables (eg, sex, age, laboratory parameters) while excluding all identifiers. As this minimal-risk observational study involved no pharmacological interventions, treatment alterations, individual result disclosure, or additional follow-up, it posed no impact on patient rights.

Therefore, the Ethics Committee approved waiver of informed consent for gout patients based on four ethical criteria: minimal risk profile, irreversible de-identification of data, absence of additional interventions, and operational impracticability of retrospective consent.

Data Security and Privacy Protection

All datasets were assigned unique coded identifiers and stored on encrypted servers with role-based access restricted to study personnel. No participant tracing or contact occurred. All samples and data were exclusively utilized for this protocol, with explicit prohibitions against disclosure, transfer, or commercial use. Upon study completion, all materials will be archived or destroyed per the regulations of our hospital and the Ethics Committee.

Data Collection

A standardized protocol integrating structured questionnaires and electronic medical records was implemented to systematically collect baseline data from all participants. Comprehensive data acquisition encompassed demographic characteristics [age, sex, body mass index (BMI)], lifestyle factors (smoking status, alcohol consumption, dietary patterns, physical activity), laboratory parameters [serum uric acid, creatinine, lipid profiles, C-reactive protein (CRP)], and immune-inflammatory markers, including IL-1β (Catalog No.ab217608, Abcam, Cambridge, UK), IL-6 (ab281515, Abcam), TNF-α (ab309419, Abcam), and NLRP3 (ab274401, Abcam), with a detection limit of 0.5 pg/mL and intra-assay variability below 10%. A total of nine biomarkers were selected for inclusion in the final predictive model (hs-CRP, CRP, IL-1β, IL-6, Th17 cells, NLRP3, CD4+/CD8+ ratio, TNF-α, and CD14++CD16+ monocytes).

Structured questionnaires included lifestyle variables (smoking, alcohol, dietary intake, physical activity), though these were not integrated into the current predictive modeling.

Unsupervised hierarchical clustering with Euclidean distance and Ward's linkage was applied. Optimal cluster number was determined by the silhouette index.

Machine Learning Modeling

This study employed multiple supervised machine learning algorithms to identify key immune factors associated with gout and develop predictive models. All analyses were conducted in R (version 4.2.3), with all immune variables standardized via Z-score normalization [mean = 0, standard deviation (SD) = 1] prior to modeling.

Feature selection integrated LASSO regression with 5-fold cross-validation to determine the optimal regularization parameter λ using the glmnet package in R. Variables retaining non-zero coefficients at the optimal λ were selected as candidate features. To enhance robustness, RF analysis was concurrently performed via the randomForest package, where variable importance were ranked. The contribution of variables to the model was assessed based on their mean decrease in Gini index. Final feature inclusion required consensus between LASSO and RF selection.

Predictive modeling encompassed XGBoost and multivariate logistic regression. The XGBoost model was optimized through grid search and 5-fold cross-validation on the training set using the xgboost package, with hyperparameter tuning targeting maximum tree depth, learning rate, subsample ratio, and iteration count. The logistic regression model was implemented via the glm function, incorporating selected features. Hyperparameters for XGBoost included maximum depth = 6, learning rate = 0.05, subsample ratio = 0.8, and 200 boosting rounds.

The dataset was partitioned into training (70%) and test (30%) sets using the caret package, ensuring balanced class distribution. Internal validation employed 5-fold cross-validation with 5 repeats, while external validation utilized an independent cohort to assess model's generalizability and stability.

Model performance was evaluated using accuracy, sensitivity, specificity, and area under the receiver operating characteristic (ROC) curve (AUC), quantified through the pROC and caret packages. Then, relevant visual charts were generated and outputted.

For enhancement of interpretability, SHapley Additive exPlanations (SHAP) analysis was conducted to explain the feature contributions of the XGBoost model. Using the SHAPforxgboost package, the SHAP values for each variable were calculated to generate feature importance bar and distribution plots, elucidating the magnitude and directionality of key immune factors' contributions to predictions, thereby facilitating subsequent biological interpretation and clinical translation (Figure S1).

Statistical Analysis

All statistical analyses were performed using SPSS version 26.0 (IBM Corp., Armonk, NY, USA) and R software version 4.2.3 (R Foundation for Statistical Computing, Vienna, Austria). SHAP values were computed using the iml package (version 0.11.2), and principal component analysis (PCA) was performed with the FactoMineR (version 2.8) and factoextra (version 1.0.7) packages, with visualization performed in GraphPad Prism version 10 (GraphPad Software, USA). Missing data were handled using multiple imputation by chained equations (MICE). All machine learning models were trained using 5-fold cross-validation repeated 5 times to reduce overfitting. Hyperparameters (eg, tree depth = 6, learning rate = 0.05, number of rounds = 200) were tuned via grid search. Model stability was further confirmed by external validation. Descriptive statistics were initially conducted, with normally distributed continuous variables expressed as mean ± SD and non-normally distributed variables reported as median (P25, P75). Comparisons for continuous variables were analyzed using independent samples t-tests or Mann–Whitney *U*-tests, as appropriate, while categorical variables were evaluated via chi-square (χ^2) tests. Multivariable logistic regression analysis was employed to assess the independent predictive capacity of selected variables, with statistical significance defined as a P-value < 0.05.

Results

Comparison of Baseline Characteristics

Among the 130 enrolled participants, the control (n=65) and gout groups (n=65) demonstrated no statistically significant differences in most baseline characteristics, indicating balanced demographic and lifestyle profiles between cohorts (all $P > 0.05$). Comparable variables included age, BMI, serum creatinine, fasting blood glucose, lipid profiles [triglycerides, total cholesterol, high-density lipoprotein cholesterol (HDL-C), low-density lipoprotein cholesterol (LDL-C)], urinary red blood cell (RBC) counts, sex distribution, residential area, educational attainment, occupational categories, smoking history, alcohol consumption, red meat/seafood intake frequency, and physical activity levels.

Notably, inflammatory biomarkers exhibited marked disparities. CRP levels were significantly elevated in the gout group [median 5.36 mg/L, interquartile range (IQR): 4.43–6.27] compared to controls (median 2.78 mg/L, IQR: 1.5–3.89; $Z = 7.627$, $P < 0.001$). Similarly, high-sensitivity CRP (hs-CRP) levels were higher in gout patients (median 5.19 mg/L vs 1.05 mg/L in controls; $Z = 9.818$, $P < 0.001$), consistent with heightened systemic inflammation in the disease cohort. Furthermore, serum uric acid levels were significantly increased in gout patients (332.04 ± 47.62 μmol/L) relative to controls (254.10 ± 34.54 μmol/L; $t = 10.681$, $P < 0.001$, Table 1), aligning with the metabolic hallmarks of gout pathophysiology.

Comparison of Immunological Biomarkers

Comparative analysis of immunological biomarkers revealed significant inflammatory activation and immune dysregulation in the gout cohort relative to controls (Table 2, Figure 1). IL-6 levels were markedly elevated in gout patients (median: 2.94 pg/mL vs 0.74 pg/mL in controls; $Z = 4.237$, $P < 0.001$), indicating systemic inflammatory activation. Similarly, IL-1β concentrations were significantly higher in the gout group (median: 1.16 pg/mL vs 0.33 pg/mL; $Z = 4.886$, $P < 0.001$), reinforcing the pivotal role of proinflammatory cytokines in gout pathogenesis.

The relative expression of the NLRP3 gene was notably increased in gout patients (median: 2.16 vs 0.38 in controls; $Z = 4.930$, $P < 0.001$), suggesting NLRP3 inflammasome activation as a central driver of immune responses in gout. Furthermore,

 https://doi.org/10.2147/JIR.S549357

Table 1 Comparison of Baseline Characteristics

Variable		Control Group (n = 65)	Gout Group (n = 65)	Z/t/χ^2	*P*
Age (years)		52.77 ± 6.48	52.94 ± 7.45	0.138	0.89
BMI (kg/m²)		26.62 ± 4.36	25.31 ± 4.24	−1.743	0.084
Serum uric acid (μmol/L)		254.10 ± 34.54	332.04 ± 47.62	10.681	0
Serum creatinine (μmol/L)		86.41 ± 14.75	85.58 ± 14.98	−0.317	0.752
Fasting blood glucose (mmol/L)		3.41 ± 0.97	3.49 ± 0.96	0.517	0.606
Triglycerides (mmol/L)		1.28 ± 0.46	1.35 ± 0.48	0.86	0.391
Total cholesterol (mmol/L)		4.03 ± 0.68	4.21 ± 0.78	1.351	0.179
HDL-C (mmol/L)		1.69 ± 0.29	1.68 ± 0.27	−0.221	0.826
LDL-C (mmol/L)		2.11 ± 0.74	2.15 ± 0.78	0.35	0.727
CRP (mg/L)		2.78 (1.5, 3.89)	5.36 (4.43, 6.27)	7.627	0
hs-CRP (mg/L)		1.05 (0.64, 1.63)	5.19 (4.41, 5.62)	9.818	0
Urinary RBC count		2 (1, 4)	2 (1, 4)	0	1
Sex	Male	34 (52.31%)	35 (53.85%)	0.031	0.860
	Female	31 (47.69%)	30 (46.15%)		
Residential area	Rural	32 (49.23%)	37 (49.23%)	0.772	0.380
	Urban	33 (49.23%)	28 (49.23%)		
Educational level	Primary school or below	16 (24.62%)	15 (23.08%)	0.123	0.989
	Middle school	15 (23.08%)	16 (24.62%)		
	High school	18 (27.69%)	17 (26.15%)		
	College or above	16 (24.62%)	17 (26.15%)		
Occupation	Retired	21 (32.31%)	19 (29.23%)	0.800	0.849
	Sedentary	14 (21.54%)	18 (27.69%)		
	Manual labor	19 (29.23%)	19 (29.23%)		
	Others	11 (16.92%)	9 (13.85%)		
Smoking history	Yes	29 (44.62%)	31 (47.69%)	0.124	0.725
	No	36 (55.38%)	34 (52.31%)		
Alcohol consumption	Yes	23 (35.38%)	32 (49.23%)	2.553	0.110
	No	42 (64.62%)	33 (50.77%)		
Red meat intake frequency	Daily	8 (12.31%)	6 (9.23%)	2.250	0.522
	Weekly	32 (49.23%)	38 (58.46%)		
	Occasionally	18 (27.69%)	12 (18.46%)		
	Never	7 (10.77%)	9 (13.85%)		
Seafood intake frequency	Daily	9 (13.85%)	7 (10.77%)	2.676	0.444
	Weekly	17 (26.15%)	12 (18.46%)		
	Occasionally	24 (36.92%)	33 (50.77%)		
	Never	15 (23.08%)	13 (20.0%)		
Physical activity frequency	Regularly	22 (33.85%)	16 (24.62%)	1.344	0.511
	Occasionally	31 (47.69%)	35 (53.85%)		
	Never	12 (18.46%)	14 (21.54%)		

Abbreviations: BMI, Body mass index; HDL-C, High-density lipoprotein cholesterol; LDL-C, Low-density lipoprotein cholesterol; CRP, C-reactive protein; hs-CRP, High-sensitivity CRP; RBC, Red blood cell.

Table 2 Comparison of Immunological Biomarkers Between Gout and Control Groups

Variable	Control Group	Gout Group	Z/t	*P*
IL-6 (pg/mL)	0.7355 (0.2194, 1.201)	2.9404 (0.2088, 4.9137)	4.237	0
TNF-α (pg/mL)	0.5068 (0.266, 0.7407)	1.3334 (0.01, 3.9229)	1.485	0.138
NLRP3 (relative mRNA level)	0.3807 (0.01, 0.9457)	2.1565 (0.4471, 4.7669)	4.93	0
$CD4^+/CD8^+$	0.3324 (0.0249, 0.5827)	1.5214 (0.1533, 3.0212)	4.778	0

(*Continued*)

Table 2 (Continued).

Variable	Control Group	Gout Group	Z/t	*P*
$CD14^+/CD16^+$	0.815 (0.353, 1.733)	2.8026 (0.1711, 6.5737)	3.796	0
IL-1β (pg/mL)	0.3259 (0.1483, 0.6305)	1.1608 (0.3265, 2.0185)	4.886	0
Th17/Treg	0.414 (0.0202, 0.9757)	2.683 (0.01, 5.3293)	4.243	0

Abbreviations: IL-6, Interleukin-6; TNF-α, Tumor necrosis factor-α; NLRP3, NLR family pyrin domain-containing 3; IL-1β, Interleukin-1β; Treg, Regulatory T-cell.

the $CD4^+/CD8^+$ T-cell ratio (median: 1.52 vs 0.33; Z = 4.778, $P < 0.001$) and Th17/Treg ratio (median: 2.68 vs 0.41; Z = 4.243, $P < 0.001$) were significantly elevated in the gout cohort, reflecting T-cell subset imbalance and a proinflammatory shift toward Th17 dominance, indicative of aberrant adaptive immune regulation. Among monocyte subpopulations, $CD14^+/CD16^+$ cell levels were substantially higher in gout patients (median: 2.80 vs 0.82; Z = 3.796, $P < 0.001$), implicating proinflammatory monocytes in localized or systemic inflammatory processes during gout flares. Although TNF-α levels trended upward in the gout group, the difference lacked statistical significance (Z = 1.485, $P = 0.138$).

Collectively, these findings demonstrate pronounced elevations in proinflammatory mediators, immune cell subset imbalances, and inflammasome activation in gout patients, underscoring the critical involvement of immune-inflammatory mechanisms in disease pathophysiology.

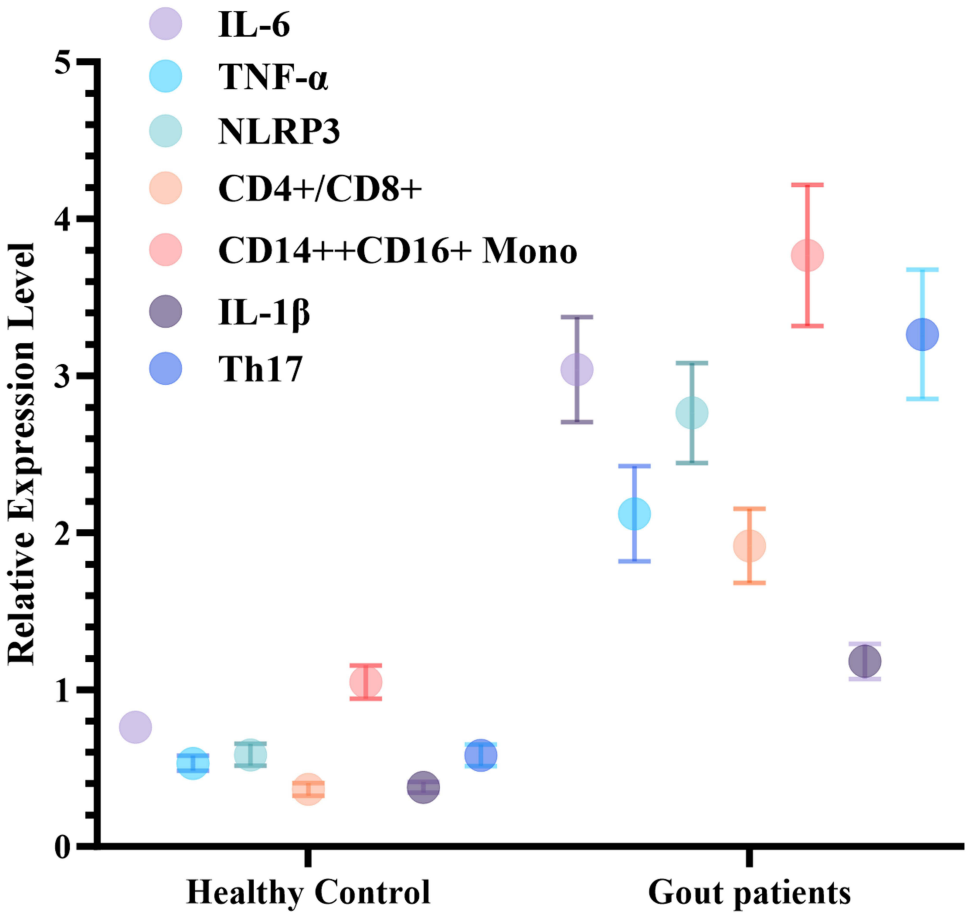

Figure 1 A boxplot for expression levels of immune factors between groups. Control (n=65) and gout groups (n=65). The figure illustrates differences in key immune biomarkers, including interleukin-1β (IL-1β), interleukin-6 (IL-6), tumor necrosis factor-α (TNF-α), NLR family pyrin domain-containing 3 (NLRP3), and $CD4^+/CD8^+$ T-cell ratios, between gout patients and controls. Data are presented as mean ± standard error of the mean (SEM).

https://doi.org/10.2147/JIR.S549357

Specific Immunological Signature Variations in Gout Patients

Cluster analysis (Figure 2) identified two distinct immunological subtypes among gout patients. The first subtype was characterized by elevated levels of proinflammatory cytokines, including TNF-α, IL-6, NLRP3, and IL-1β. These patients exhibited pronounced neutrophil infiltration, hallmark acute gout flare symptoms, enhanced NLRP3 inflammasome activity driving cytokine production, and hyperactivation of monocytes/macrophages with predominant M1 polarization. Clinically, this group showed recurrent acute flares with intense but transient inflammatory responses. The second subtype was marked by Th17 dominance, T-cell subset imbalance (eg, Th17/Treg disequilibrium), and B-cell dysfunction, accompanied by chronic low-grade inflammation. These patients frequently presented with tophi formation, progressive joint destruction, and impaired Treg-mediated immunoregulation. Despite fewer acute episodes, this subtype demonstrated sustained tissue damage progression. These findings suggest that combinatorial immune biomarker profiles may enable immunological subtyping and personalized risk stratification in gout management.

Construction of an Immunological Factor-Based Gout Risk Prediction Model (Model Flowchart and Feature Importance bar Plot)

As shown in Figure 3, LASSO regression was employed to identify key immunological variables for the gout diagnostic model. With increasing λ values, coefficients for most variables progressively shrank toward zero, retaining only those with substantial contributions. The final model selected seven non-zero coefficient variables: IL-1β, IL-6, NLRP3, TNF-α, $CD4^+/CD8^+$ T-cell ratio, $CD14^{++}CD16^+$ monocytes, and Th17/Treg ratio. Cross-validation curves (Figure 4 and Table 3) confirmed model stability and parsimony at both lambda.min and lambda.1se, with both corresponding to the same seven retained variables, indicating robust generalizability.

XGBoost-Based Prediction Model for Immunological Factors and Internal Validation

Following variable selection via LASSO regression, SHAP analysis (Figure 5) identified IL-1β, IL-6, and the $CD4^+/CD8^+$ ratio as the most influential predictors. An XGBoost binary classification model was constructed using the seven retained immune biomarkers: IL-1β, IL-6, NLRP3, TNF-α, $CD4^+/CD8^+$ T-cell ratio, $CD14^{++}CD16^+$ monocytes, and Th17/Treg ratio. The dataset was partitioned into training (70%) and testing (30%) subsets. The confusion matrix (Figure 6) further confirmed the model's precision (accuracy 100%), revealing no instances of misclassification or omission. These findings underscore the model's capacity to leverage immune biomarker profiles for precise disease stratification.

Stable Model Performance in an Independent Validation Cohort (External Validation by ROC Curve Analysis)

The external validation cohort included 48 patients, with baseline demographics comparable to the discovery cohort (Table S1). Baseline characteristics of the external validation cohort (24 gout patients and 24 healthy controls) were comparable to those of the discovery cohort (65 gout patients and 65 controls). No statistically significant differences were observed across demographic, metabolic, or inflammatory indicators (all $P > 0.05$), supporting the representativeness of the validation cohort (Table S1). External validation using an independent hospital-based cohort (n = 48) demonstrated robust generalizability of the model, achieving an AUC of 0.977, accuracy of 93.75%, sensitivity of 95.83% [effective identification of positive class (Label = 1)], and specificity of 91.67% [accurate classification of negative class (Label = 0)], with all metrics exceeding 85% (Figure 7). These results confirm the model's stability and potential utility in preclinical screening, highlighting its capacity to maintain high diagnostic fidelity across heterogeneous populations. The combined internal and external validation outcomes underscore the clinical translatability of this immune biomarker-driven predictive framework.

Integration of Inflammatory and Immune Biomarkers in Logistic Regression Analysis and Model Optimization

Building on univariate analyses, multivariable binary logistic regression incorporating all candidate variables was performed to identify independent predictors. Although the overall model achieved statistical significance, *P*-values of

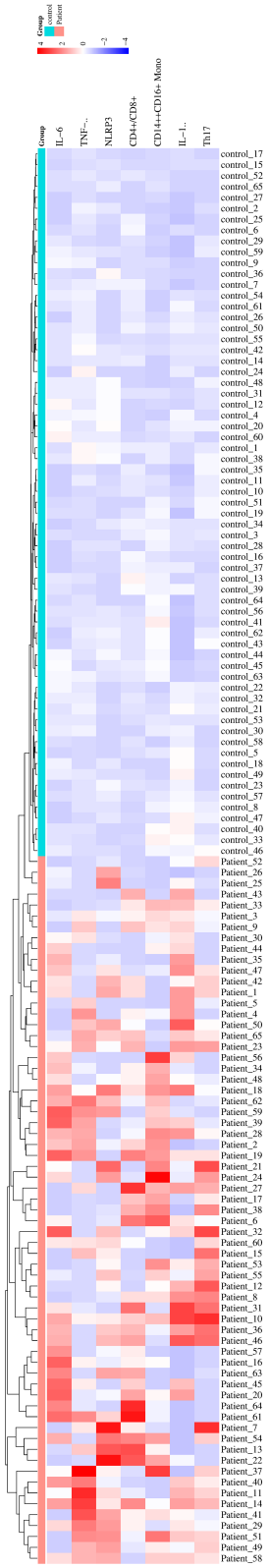

Figure 2 Cluster heatmap for immune profiling. Hierarchical clustering analysis illustrates distinct immunological patterns based on cytokine and immune cell subset expression profiles. Heatmap colors represent Z-score standardized expression levels.

https://doi.org/10.2147/JIR.S549357

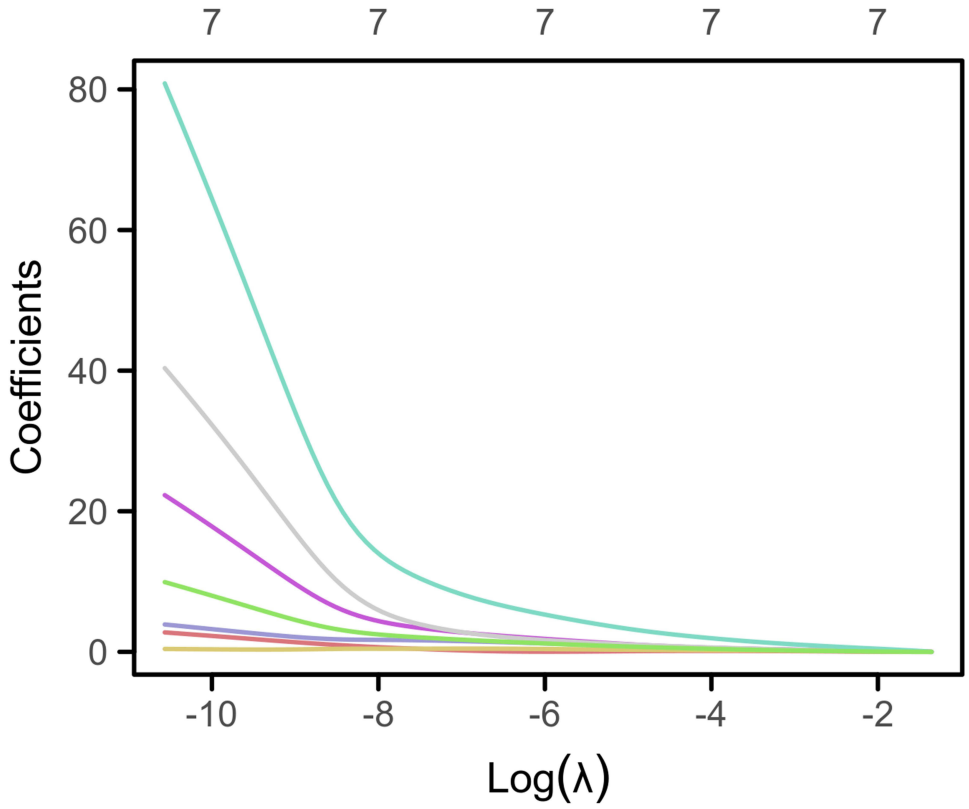

Figure 3 LASSO regression coefficient trajectory. The x-axis represents log-transformed λ values [log(λ)], and the y-axis denotes variable coefficients. Each trajectory illustrates the coefficient evolution of a predictor as λ increases.

individual variables approached 1, suggesting no significant independent risk factors. This likely reflects pronounced multicollinearity among variables, which undermined model stability and inflated variance (Tables 4 and 5).

To screen key immune factors in gout patients, descriptive statistics and distribution visualization of raw data were performed, revealing approximately normal distributions for most variables, with minor outliers observed for IL-1β and Th17 (Figure 8). No zero-inflation issues were detected (proportion of zeros < 0.01% for all variables).

To address collinearity, LASSO regression with cross-validation identified nine stable predictors, ranked by coefficient magnitude: hs-CRP (10.09), Th17 (3.08), $CD4^+/CD8^+$ (2.61), CRP (2.53), IL-6 (1.62), IL-1β (1.10), TNF-α (1.06), $CD14^{++}CD16^+$ monocytes (0.73), and NLRP3 (0.07), as listed in Table 6.

PCA was subsequently applied for dimensionality reduction to mitigate multicollinearity. The loading matrix revealed that principal component 1 (PC1) was predominantly influenced by CRP, hs-CRP, IL-6, and Th17, PC3 exhibited the highest weighting for IL-1β, while PC4 was dominated by TNF-α, underscoring the critical contributions of these variables to model construction. The PCA cumulative explained variance plot demonstrated that the first three principal components together explained about 70% of the total variance, whereas five components captured approximately 87%. Beyond the fifth component, the incremental gain in explained variance diminished, with all seven components accounting for >95% of the variability. These findings suggest that selecting four to five components achieves an optimal balance between dimensionality reduction and information retention. (Table 7 and Figure 9).

RF analysis corroborated LASSO results, ranking hs-CRP as the most critical predictor (importance score: 0.559), followed by CRP (0.108), IL-1β (0.079), and IL-6 (0.062), with Th17, NLRP3, and $CD4^+/CD8^+$ also demonstrating predictive relevance (Table 8 and Figure 10). A final model integrating these key variables achieved flawless discrimination [AUC = 0.981, accuracy = 100%, sensitivity (Recall, label 1) = 100%, specificity (Recall, label 0) = 100%] (Figure 11), underscoring their pivotal roles in gout immunopathogenesis.

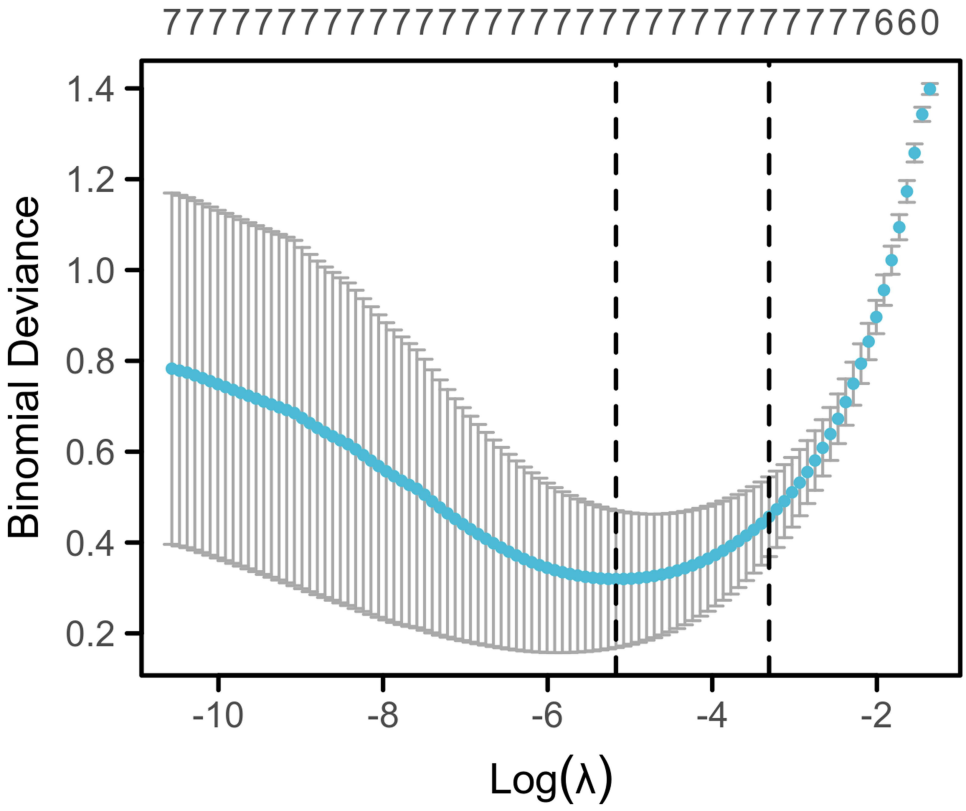

Figure 4 LASSO cross-validation curve. Optimal λ is selected via 10-fold cross-validation. The x-axis shows log(λ), while the y-axis displays mean squared error (MSE) or model deviance. Dots indicate average MSE per λ, with error bars representing standard error (SE). Vertical dashed lines denote lambda.min (left, minimal MSE) and lambda.1se (right, most parsimonious model within one SE).

Discussion

This study compared patients with gout to healthy control individuals, offering a clear contrast for identifying biomarker differences, although it does not fully capture the complexity of real-world patients with multiple comorbidities. Within this framework, our analysis systematically delineates the immunoinflammatory landscape of gout, revealing marked systemic inflammatory activation and immune cell subset dysregulation, findings that are consistent with and extend established literature. Previous investigations have documented elevated circulating proinflammatory cytokines and obvious T-cell subset perturbations in gout populations.[25,26] Through LASSO regression, seven pivotal immune factors were identified, forming the basis of an XGBoost predictive model. This model demonstrated exceptional discriminatory capacity in both internal validation and independent cohorts (AUC approaching 1.0), underscoring robust generalizability.[27,28] Cluster analysis further stratified gout patients into two immunophenotypically distinct subtypes: one characterized by proinflammatory factor hyperactivation and the other by T-cell subset imbalance. This dichotomy corroborates emerging theories positing an "inflammatory-autoimmune continuum" in metabolic arthropathies,[29] highlighting pathobiological heterogeneity within the gout spectrum.

Table 3 LASSO Coefficient Selection

	Lambda Value	Index	Mean Squared Error (MSE)	Standard Error (SE)	Non-Zero Coefficients
Lambda.min	0.0056839	42	0.31949	0.15064	7
Lambda.1se	0.036537	22	0.45679	0.087785	7

Notes: lambda.min: The λ value corresponding to the minimum mean squared error (MSE) of the target parameter. lambda.1se: The largest λ value within one standard error (SE) of the minimum MSE, prioritizing model simplicity. Index: Position of lambda.min and lambda.1se within the candidate λ sequence. LASSO serves as a feature selection method. If excessive variables are retained, subsequent multivariable logistic regression can optimize variable inclusion for model construction.

https://doi.org/10.2147/JIR.S549357

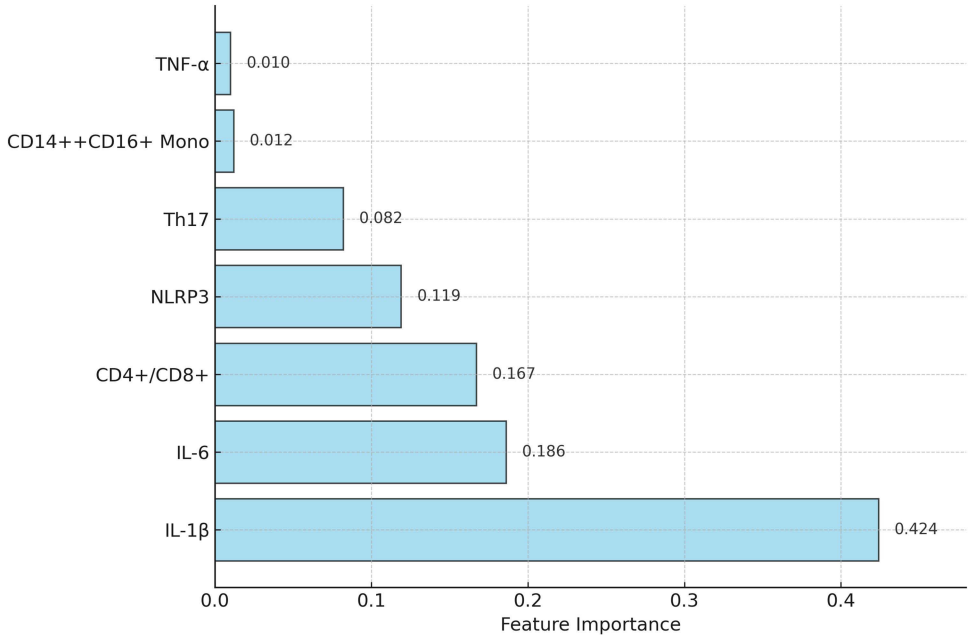

Figure 5 Bar plot of SHAP feature importance. The bar plot evaluates the contribution of feature variables to predictions in the XGBoost-based gout diagnostic model using SHAP analysis. Each bar corresponds to the mean absolute SHAP value of a variable, quantifying its relative impact on model decisions.

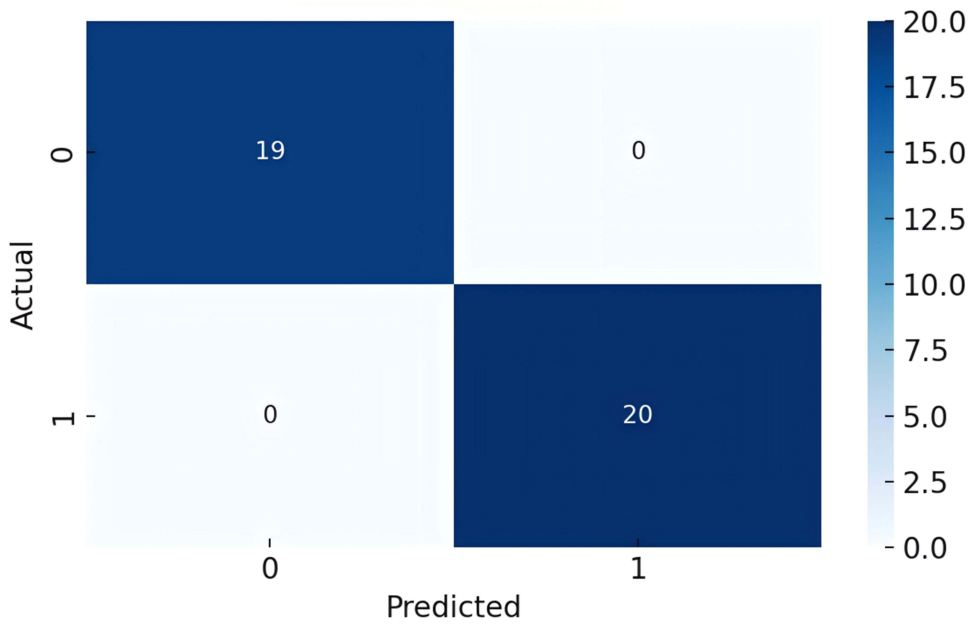

Figure 6 Confusion matrix. Performance of the XGBoost model is evaluated on the testing subset, demonstrating 100% classification accuracy with no false positives or negatives.

Mechanistically, pronounced elevations in IL-1β and NLRP3 observed in our study implicate the NLRP3 inflammasome as a central orchestrator of acute gout flares. This pathway drives proinflammatory cytokine activation and release, ultimately culminating in leukocyte infiltration in joint synovial fluid and local inflammatory response, which is a pathomechanism extensively validated across animal and clinical studies.[30,31] Concurrent upregulation of IL-6, CRP, and hs-CRP reinforces the paradigm of systemic chronic low-grade inflammation in gout, consistent with reported roles of IL-6 in urate-associated inflammatory modulation.[32] hs-CRP outperformed inflammasome-specific markers, likely

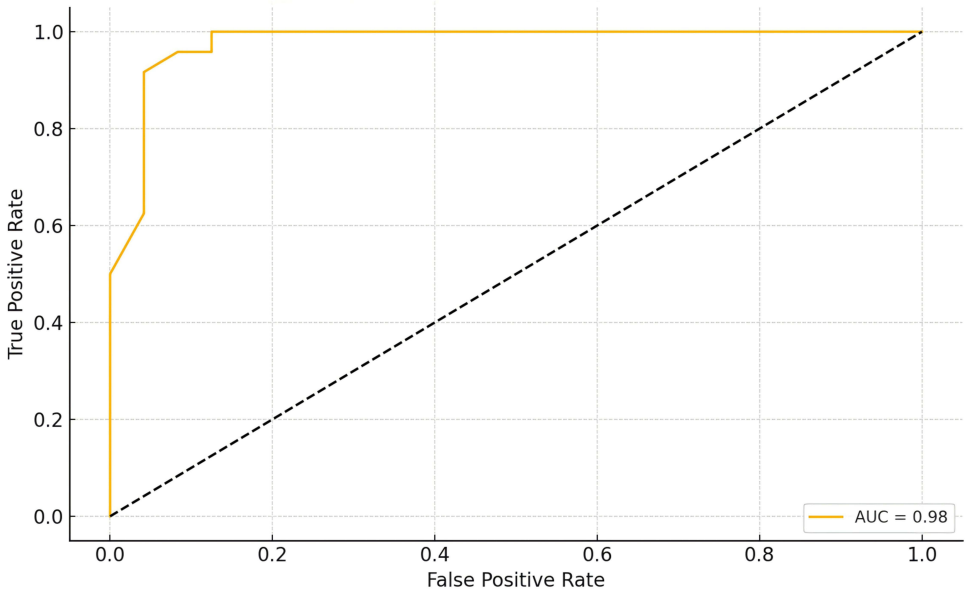

Figure 7 Model performance metrics (AUC, sensitivity, specificity). The figure compares the XGBoost model's discriminative performance in both internal cross-validation and external independent validation cohorts, emphasizing its consistency and reliability.

reflecting the dominant influence of systemic acute-phase responses over localized inflammasome activation. However, interleukin assays remain costly and technically demanding, limiting routine use. This work should be framed as exploratory, requiring prospective validation and cost-effectiveness analyses before clinical adoption. In future,

Table 4 Variable Coding for Binary Logistic Regression

Variable	Coding
Group	Control = 0, Gout = 1
IL-6 (pg/mL)	Continuous
TNF-α (pg/mL)	Continuous
NLRP3 (relative mRNA level)	Continuous
$CD4^+/CD8^+$	Continuous
$CD14^+/CD16^+$	Continuous
IL-1β (pg/mL)	Continuous
Th17/Treg	Continuous
CRP (mg/L)	Continuous
hs-CRP (mg/L)	Continuous

Table 5 Independent Risk Factor Analysis via Binary Logistic Regression

	b	SE	Wald	*P*-value	OR	95% CI
IL-6	1.990	1400.173	0.000	0.999	7.317	0.000
TNF-α	1.413	1940.565	0.000	0.999	4.107	0.000
NLRP3	0.654	2590.791	0.000	1.000	1.923	0.000
$CD4^+/CD8^+$	4.769	3071.524	0.000	0.999	117.797	0.000
$CD14^{++}CD16^+$ Mono	1.008	1725.455	0.000	1.000	2.741	0.000
IL-1β	4.618	5774.343	0.000	0.999	101.339	0.000
Th17	3.637	949.670	0.000	0.997	37.991	0.000
CRP	2.637	1711.884	0.000	0.999	13.964	0.000
hsCRP	12.148	2562.611	0.000	0.996	188,772.968	0.000
Constant	−66.611	8676.946	0.000	0.994	0.000	-

https://doi.org/10.2147/JIR.S549357

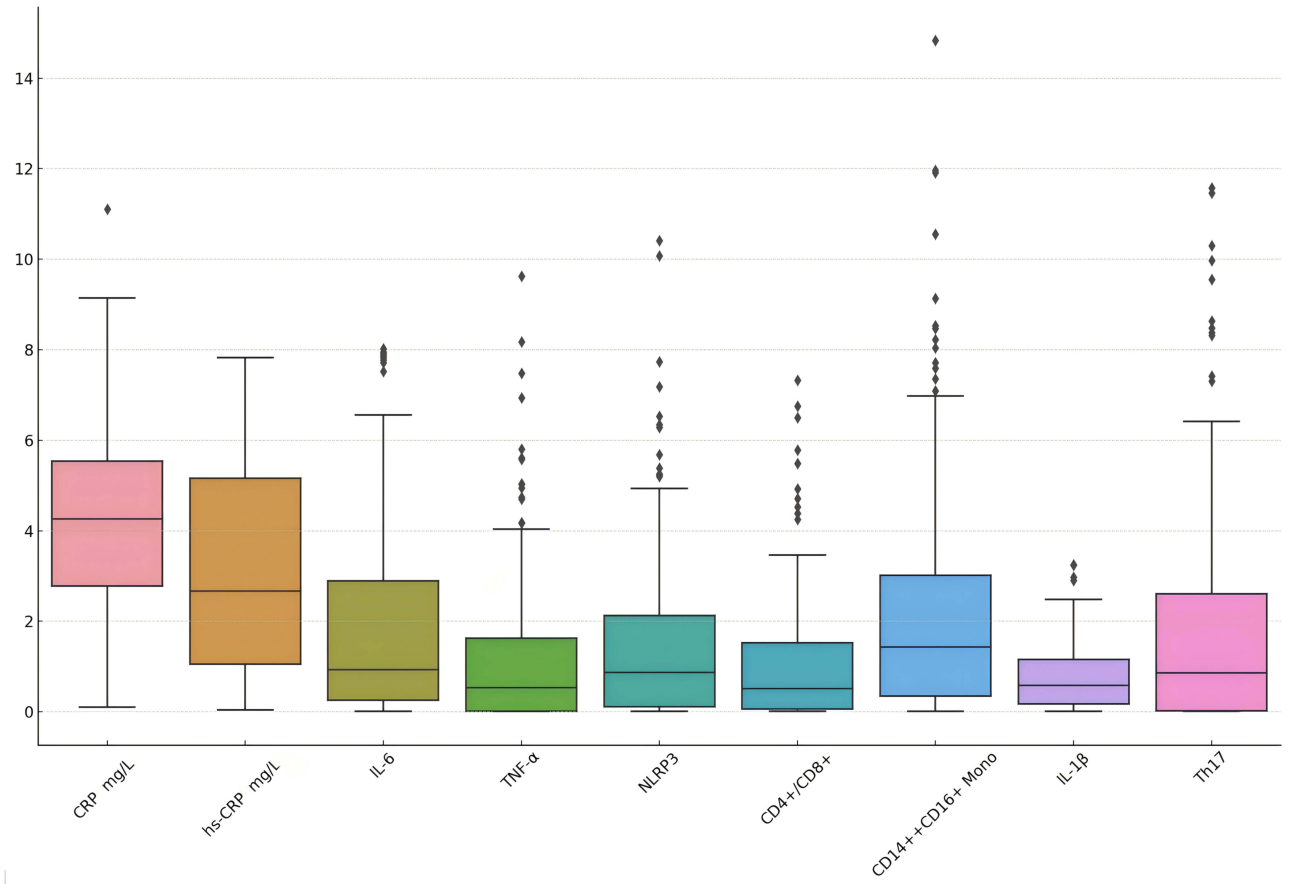

Figure 8 Variable distribution analysis. Boxplots illustrate the distribution patterns and outlier profiles of immune-inflammatory biomarkers.

biomarker-driven stratification could guide targeted therapies such as IL-1β inhibitors versus IL-6 blockade. The gout cohort as a whole exhibited significant inflammatory activation; however, subgroup analysis indicated that acute gout patients showed pronounced pro-inflammatory responses, whereas chronic gout patients displayed low-grade but sustained inflammation.

Beyond cytokine dysregulation, profound T-cell subset abnormalities emerged as hallmark features in this study. Elevated Th17/Treg ratios, $CD4^+/CD8^+$ imbalance, and $CD14^+/CD16^+$ monocyte expansion suggest coordinated involvement of adaptive immunity and the mononuclear phagocyte system in gout pathogenesis. These observations resonate with prior work detailing Th17-mediated crystal-driven inflammation[33] and synovial monocyte activation in gout.

Table 6 LASSO Regression Coefficients

Variable	LASSO Coefficient
hs-CRP	10.09
Th17	3.08
$CD4^+/CD8^+$	2.61
CRP	2.53
IL-6	1.62
IL-1β	1.1
TNF-α	1.06
$CD14^{++}CD16^+$ Mono	0.73
NLRP3	0.07

Table 7 Principal Component Loading Matrix Analysis

	PC1	PC2	PC3	PC4	PC5	PC6	PC7	PC8
CRP(mg/L)	0.40	−0.11	0.11	−0.23	0.23	0.15	0.73	−0.01
hs-CRP(mg/L)	0.47	0.05	−0.03	−0.02	−0.03	−0.15	0.22	0.33
IL-6	0.30	−0.53	0.07	−0.02	−0.23	−0.67	−0.12	−0.30
TNF-α	0.24	−0.32	−0.30	0.72	0.34	0.27	−0.05	−0.18
NLRP3	0.29	0.37	−0.49	0.22	−0.50	−0.10	0.01	0.29
$CD4^{+}/CD8^{+}$	0.32	−0.31	0.06	−0.29	−0.46	0.64	−0.28	−0.10
$CD14^{++}CD16^{+}$ Mono	0.29	0.06	−0.39	−0.47	0.55	−0.07	−0.46	0.10
IL-1β	0.30	0.09	0.68	0.26	0.13	−0.01	−0.33	0.43
Th17	0.33	0.60	0.19	0.04	0.01	−0.01	−0.07	−0.69

It is worth noting that although TNF-α failed to achieve statistical significance in population analysis, it showed an upward trend in some gout patients, suggesting that it may still have a potential context-dependent role in specific subtypes of patients, analogous to those has been observed in connective tissue diseases and other metabolism-related joint diseases,[34] warranting subtype-specific investigation. Although TNF-α did not reach independent significance in univariate testing, it was retained in the final multivariate model because of its additive contribution to predictive performance in combination with other biomarkers.

The XGBoost model's superior performance across multiethnic cohorts was complemented by SHAP analysis, which identified IL-1β, IL-6, and $CD4^{+}/CD8^{+}$ ratio as dominant predictive feature. These findings mechanistically congruent with aforementioned pathways.[35,36] The repeated validation of these immune factors in multiple independent cohorts further supports their clinical value as potential diagnostic and subtype classification biomarkers. Rigorous variable selection integrating LASSO, PCA, and RF methodologies mitigated multicollinearity while enhancing model interpretability and stability. Compared with traditional logistic regression models, XGBoost demonstrates stronger adaptability and predictive performance in handling non-linear, high-dimensional data, making it suitable for risk modeling of immunologically complex diseases such as gout.

The clinical value of the model lies in its potential applications for the early identification, risk assessment, and formulation of individualized treatment plans for individuals with hyperuricemia, patients with atypical symptoms, or

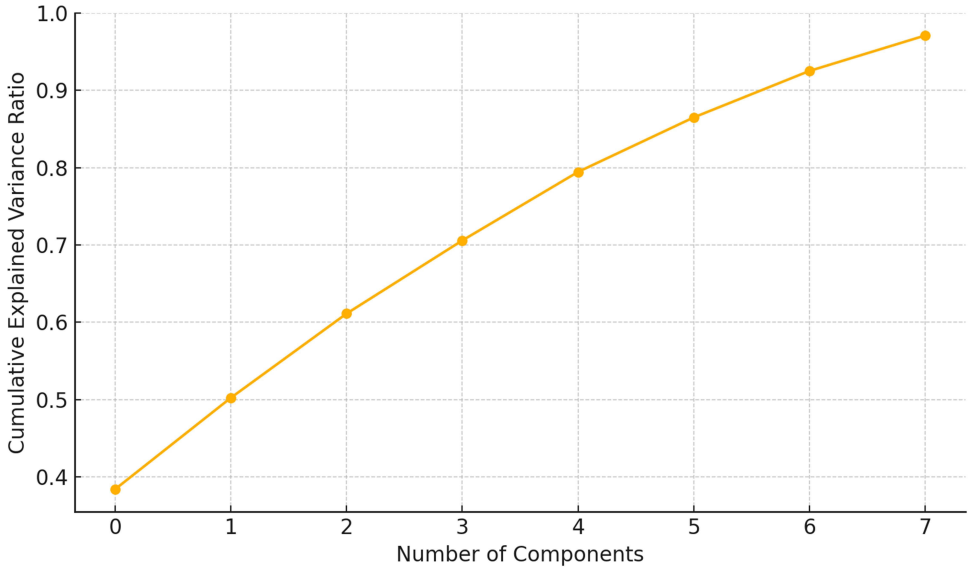

Figure 9 Principal component analysis (PCA) plot. The curve depicts the cumulative proportion of variance explained as a function of the number of retained principal components. The first three components accounted for approximately 70% of the total variance, while five components explained nearly 87%. Inclusion of all seven components captured over 95% of the variance, indicating that most of the variability in the dataset can be summarized by a limited number of principal components.

https://doi.org/10.2147/JIR.S549357

Table 8 Variable Importance Ranking by Random Forest

Rank	Variable	Importance Score
1	hs-CRP(mg/L)	0.559
2	CRP(mg/L)	0.108
3	IL-1β	0.079
4	IL-6	0.062
5	Th17	0.055
6	NLRP3	0.045
7	$CD4^+/CD8^+$	0.043
8	TNF-α	0.026
9	$CD14^{++}CD16^+$ Mono	0.022

those without a clear history of episodes. For example, in the current context of a lack of clear immunotyping tools, this model can serve as a reference indicator to assist in assessing patients' inflammatory activity status and potential progression risk.

Although the findings of this study are innovative and have translational potential, several limitations remain. First, as this was a cross-sectional design, establishing a causal relationship is difficult and needs to be further confirmed through prospective follow-up studies. Second, the sample size and number of study centers were limited, and some indicators showed variability across different subgroups, potentially influenced by population heterogeneity. Third, the model did not incorporate variables such as uric acid, genetic factors, and lifestyle. Future research could further integrate multi-omics data (eg, transcriptomic, metabolomic) to construct a multidimensional prediction framework, thereby enhancing the model's accuracy and applicability. We acknowledge that lifestyle and medication-related factors, which are highly relevant to gout risk, were not incorporated into the final model. This omission reflects data incompleteness and warrants further exploration. Although the study duration spanned two years, the relatively modest sample size may limit generalizability. The sample size was determined a priori using power calculations based on IL-1β effect size, ensuring statistical robustness. Nevertheless, larger multicenter cohorts are warranted for external validation. Another limitation is that the gender distribution of our cohort is not typical, with a relatively lower male proportion, which may influence generalizability. The gender distribution in our cohort reflects the characteristics of our local hospitalized population,

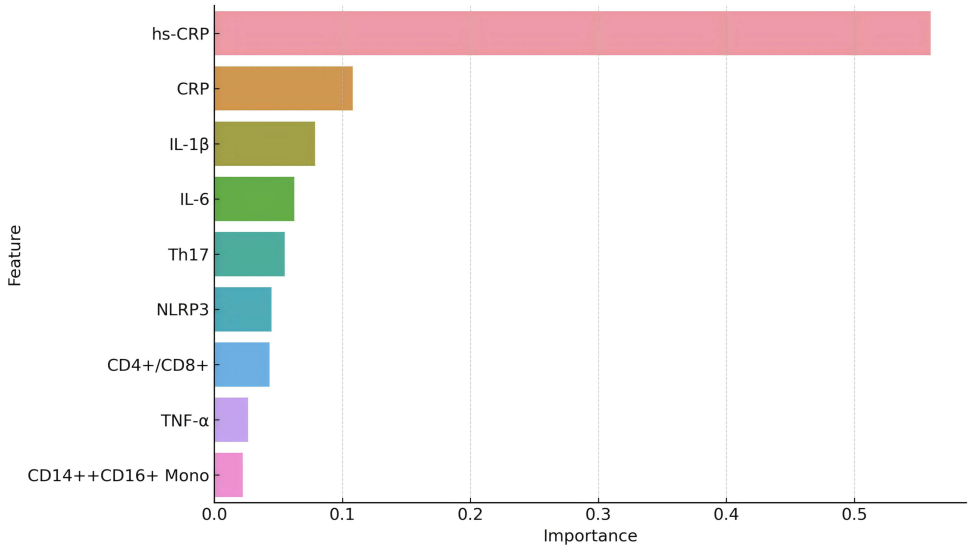

Figure 10 Variable importance ranking by random forest. The bar plot shows the relative contribution of each biomarker to the final predictive model based on random forest analysis. High-sensitivity C-reactive protein (hs-CRP) demonstrated the greatest importance, followed by CRP, IL-1β, and IL-6. Other immune-related variables, including Th17 cells, NLRP3, CD4+/CD8+ ratio, TNF-α, and CD14++CD16+ monocytes, also contributed to the model, albeit to a lesser extent.

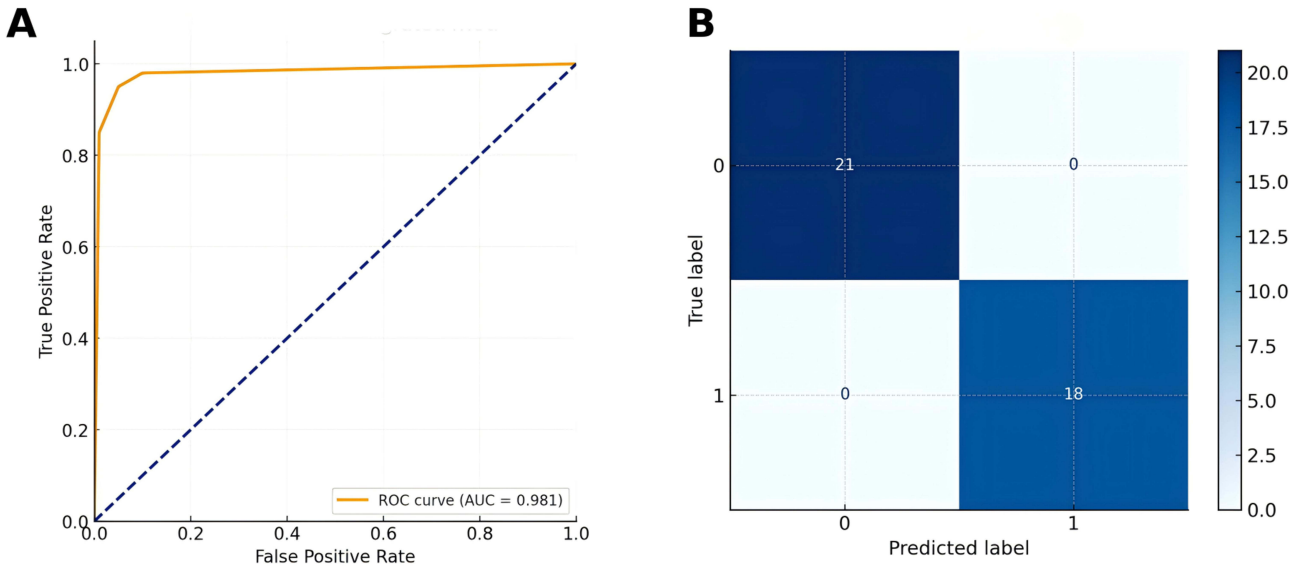

Figure 11 Performance evaluation of the final integrated prediction model. (**A**) Receiver operating characteristic (ROC) curve of the integrated model combining hs-CRP, CRP, IL-1β, IL-6, Th17 cells, NLRP3, and CD4+/CD8+ ratio. (**B**) Confusion matrix of the classification results.

where female patients more frequently seek inpatient care for gout-related complications. The relatively lower male proportion in both patient and control groups may introduce selection bias and limit the generalizability of our findings. A key limitation is the use of healthy controls rather than patients with multiple comorbidities, which may restrict the generalizability of the model as a screening tool in typical clinical practice, where gout is most often underdiagnosed among elderly individuals with complex health conditions. Our findings should also be considered in light of the broader diagnostic challenges in gout. In routine practice, many patients progress silently toward tophaceous disease due to underrecognition, misdiagnosis, or limited availability of reliable diagnostic tools. This emphasizes the clinical importance of developing and validating novel approaches that can improve early detection and guide timely intervention.

Although our model integrates multiple immunological biomarkers with strong predictive performance, several markers—such as NLRP3 expression, Th17/Treg ratios, and monocyte subsets—require specialized assays that are not yet widely available in routine clinical practice. This may limit immediate applicability due to feasibility and cost considerations. Therefore, our study should be regarded as a proof-of-concept, highlighting the need for future validation in larger and more diverse cohorts, as well as the development of simplified biomarker panels or surrogate markers that can be more easily implemented in standard workflows.

While our model demonstrates strong predictive value, its feasibility in clinical practice may be limited by the cost and accessibility of specialized immune biomarker assays. Streamlining biomarker panels and developing surrogate tests will be essential for integration into standard diagnostic workflows. Importantly, the proposed immunological subtypes may provide therapeutic insights. For example, patients with a pronounced IL-1β or NLRP3 signature may benefit more from targeted anti-inflammatory agents, whereas those with T-cell imbalance could be considered for immunomodulatory strategies.

In conclusion, this study delineates specific immune factor profiles in gout patients and establishes an immunological prediction model with high predictive performance and biological interpretability. These findings provide a theoretical foundation and methodological framework for advancing the understanding of gout's immune mechanisms, exploring stratified diagnosis and treatment strategies based on immune subtypes, and promoting individualized precision care. Future studies should expand sample size, incorporate longitudinal follow-up, and focus on clinical feasibility to accelerate the translation of these findings into practice.

Conclusion

This study delineates distinct immunoinflammatory signatures in gout and demonstrates that an XGBoost model incorporating LASSO-selected immune biomarkers achieves high predictive accuracy in both internal and external

https://doi.org/10.2147/JIR.S549357

validations. Cluster analysis further revealed immunologically heterogeneous gout subtypes, highlighting disease complexity and potential therapeutic implications. These findings support the value of immune biomarkers for risk stratification and personalized management. Nonetheless, limitations include reliance on specialized assays, the use of healthy controls rather than comorbidity-rich cohorts, and the need for larger, prospective validation. Addressing these challenges will be essential for clinical translation of this predictive framework.

Ethics Statement

This cross-sectional study was conducted in accordance with the ethical principles of the Declaration of Helsinki and approved by the Ethics Committee of the People's Hospital of Chongqing Liang Jiang New Area (Approval No.: 2025-066).

Funding

This study did not receive any funds.

Disclosure

No potential conflict of interest was reported by the author(s).

References

1. FitzGerald JD. Gout. *Ann Intern Med*. 2025;178(3):ITC33–ITC48. doi:10.7326/ANNALS-24-03951
2. Ahn EY, So MW. The pathogenesis of gout. *J Rheum Dis*. 2025;32(1):8–16. doi:10.4078/jrd.2024.0054
3. Gerard B, Leask M, Merriman TR, et al. Hyperuricaemia and gout in the Pacific. *Nat Rev Rheumatol*. 2025;21(4):197–210. doi:10.1038/s41584-025-01228-7
4. Wang Y, Dalbeth N, Terkeltaub R, et al. Target serum urate achievement and chronic kidney disease progression in patients with gout and kidney disease. *JAMA Intern Med*. 2025;185(1):74–82. doi:10.1001/jamainternmed.2024.6212
5. Zhang Y, Jin Z, Yao J, Wang D, Yu W, Zhang Y. Global, regional, and national burden of gout in people aged 15-39 years from 1990 to 2021: trends, cross-country inequalities and forecast to 2035. *Joint Bone Spine*. 2025;92(6):105929. doi:10.1016/j.jbspin.2025.105929
6. Collaborators GBDG. Global, regional, and national burden of gout, 1990-2020, and projections to 2050: a systematic analysis of the Global Burden of Disease Study 2021. *Lancet Rheumatol*. 2024;6(8):e507–e517. doi:10.1016/S2665-9913(24)00117-6.
7. Asghari KM, Zahmatyar M, Seyedi F, et al. Gout: global epidemiology, risk factors, comorbidities and complications: a narrative review. *BMC Musculoskelet Disord*. 2024;25(1):1047. doi:10.1186/s12891-024-08180-9
8. Chandratre P, Sabido-Sauri R, Zhao SS, Gout AA. Hyperuricemia and Psoriatic Arthritis: an Evolving Conundrum. *Curr Rheumatol Rep*. 2025;27(1):22. doi:10.1007/s11926-025-01187-8
9. Schlesinger N, Pillinger MH, Simon LS, Lipsky PE. Interleukin-1beta inhibitors for the management of acute gout flares: a systematic literature review. *Arthritis Res Ther*. 2023;25(1):128. doi:10.1186/s13075-023-03098-4
10. Yan LJ, Qi S, Wu C, et al. Hypocrellin A from an ethnic medicinal fungus protects against NLRP3-driven gout in mice by suppressing inflammasome activation. *Acta Pharmacol Sin*. 2025;46(4):1016–1029. doi:10.1038/s41401-024-01434-1
11. Ni X, Wang Q, Ning Y, et al. Anemoside B4 targets NEK7 to inhibit NLRP3 inflammasome activation and alleviate MSU-induced acute gouty arthritis by modulating the NF-kappaB signaling pathway. *Phytomedicine*. 2025;138:156407. doi:10.1016/j.phymed.2025.156407
12. Zhang Z, Wang P, Xiong Q, et al. Advancements in the study of IL-6 and its receptors in the pathogenesis of gout. *Cytokine*. 2024;182:156705. doi:10.1016/j.cyto.2024.156705
13. Li M, Yin ZJ, Li L, et al. Rutaecarpine attenuates monosodium urate crystal-induced gouty inflammation via inhibition of TNFR-MAPK/NF-kappaB and NLRP3 inflammasome signaling pathways. *Chin J Integr Med*. 2025. doi:10.1007/s11655-025-4204-3
14. Zi X, Su R, Su R, et al. Elevated serum IL-2 and Th17/Treg imbalance are associated with gout. *Clin Exp Med*. 2024;24(1):9. doi:10.1007/s10238-023-01253-4
15. Lai R, Deng X, Lv X, Zhong Y. Causal relationship between inflammatory proteins, immune cells, and gout: a Mendelian randomization study. *Sci Rep*. 2024;14(1):30070. doi:10.1038/s41598-024-80138-2
16. Zeng Y, Huang M, Zeng W, Lei L. The causal association between immune cells and gout: a bidirectional two-sample Mendelian randomization study. *Medicine*. 2024;103(42):e40064. doi:10.1097/MD.0000000000040064
17. Afzal M, Rednam M, Gujarathi R, Widrich J. *Gout*. StatPearls. 2025.
18. Yang Y, Liu Z. The changing burden of gout in adults aged 70 and above based on the global burden of disease 2019. *Front Public Health*. 2025;13:1455726. doi:10.3389/fpubh.2025.1455726
19. Bajad S, Tanna D, Jn DRY, Gupta R. DECT: a novel window in gout imaging. *J Assoc Physicians India*. 2023;71(6):11–12.
20. Sirotti S, Pascart T, Thiele R, Filippou G. Imaging of crystal-induced arthropathies in 2025. *Best Pract Res Clin Rheumatol*. 2025;39(3):102063. doi:10.1016/j.berh.2025.102063
21. Sekeramayi TM, Sivaprakasam T, Fanciullo J. Pseudogout in primary care practice: an approach to diagnosis and treatment. *S D Med*. 2025;78(4):177–181.
22. Lamprecht C, Turnbull L, Barnett A, Nasri E, Wang M. Steroid or pseudogout? Analysis of white deposits in tissues during surgery. *Arch Orthop Trauma Surg*. 2025;145(1):345. doi:10.1007/s00402-025-05945-2
23. Bartsch V, Standfest K, Hueber A. Gout: from the diagnosis to guideline-based treatment. *Z Gerontol Geriatr*. 2025;58(2):137–146. doi:10.1007/s00391-025-02416-6

24. Snast I, Dalal A, Twig G, et al. Acne and obesity: a nationwide study of 600,404 adolescents. *J Am Acad Dermatol*. 2019;81(3):723–729. doi:10.1016/j.jaad.2019.04.009
25. Yan J, Liu Y. Correlation of systemic immune inflammation and serum uric acid with gout: based on NHANES. *Clin Rheumatol*. 2025;44(1):425–432. doi:10.1007/s10067-024-07271-1
26. Roman Y. Correlation of systemic immune inflammation and serum uric acid with gout: based on NHANES. *Clin Rheumatol*. 2025;44(3):1393–1394. doi:10.1007/s10067-025-07329-8
27. Doyle P, Gong W, Hsi R, Kavoussi N. Machine learning models to predict kidney stone recurrence using 24 hour urine testing and electronic health record-derived features. *Res Sq*. 2023. doi:10.21203/rs.3.rs-3107998/v1
28. Lei T, Guo J, Wang P, et al. Establishment and validation of predictive model of tophus in gout patients. *J Clin Med*. 2023;12(5). doi:10.3390/jcm12051755
29. Hentschel E, Siyal S, Al Sager A, McCoy DC, Yousafzai AK. The development and validity of the early learning tool for children 0-3-year-old in rural Pakistan. *J Glob Health*. 2024;14:04241. doi:10.7189/jogh.14.04241
30. Li G, Du S, Yan S, et al. Mechanism of Biqi capsules in the treatment of gout based on network pharmacology and experimental verification. *J Ethnopharmacol*. 2025;337(Pt 1):118817. doi:10.1016/j.jep.2024.118817
31. Liu J, Liu G, Chu T, Wu Y, Yang LZ, Fang W. The progress of immune cells-induced inflammatory response in gout. *Curr Pharm Des*. 2025. doi:10.2174/0113816128369016250306050522
32. Khosravi H, Stevens V, Sanchez RH. HFIP as a versatile solvent in resorcin[n]arene synthesis. *Beilstein J Org Chem*. 2024;20:2469–2475. doi:10.3762/bjoc.20.211
33. Alaswad A, Cabau G, Crisan TO, et al. Integrative analysis reveals the multilateral inflammatory mechanisms of CD14 monocytes in gout. *Ann Rheum Dis*. 2025. doi:10.1016/j.ard.2025.01.046
34. Paviotti G, Pavan M, Driutti M, et al. Thoracic electrical bioimpedance in preterm newborns with and without respiratory distress syndrome: an exploratory observational study. *Eur J Pediatr*. 2025;184(3):208. doi:10.1007/s00431-025-06049-0
35. Xiao L, Zhao Y, Li Y, et al. Developing an interpretable machine learning model for diagnosing gout using clinical and ultrasound features. *Eur J Radiol*. 2025;184:111959. doi:10.1016/j.ejrad.2025.111959
36. Gu W, Zhao J, Xu Y. Hyperuricemia-induced complications: dysfunctional macrophages serve as a potential bridge. *Front Immunol*. 2025;16:1512093. doi:10.3389/fimmu.2025.1512093